Applied Microbiology and Biotechnology (2024) 108:547
https://doi.org/10.1007/s00253-024-13379-w

APPLIED GENETICS AND MOLECULAR BIOTECHNOLOGY

Omics-driven onboarding of the carotenoid producing red yeast *Xanthophyllomyces dendrorhous* CBS 6938

Emma E. Tobin[1] · Joseph H. Collins[1] · Celeste B. Marsan[1] · Gillian T. Nadeau[1] · Kim Mori[1] · Anna Lipzen[2] · Stephen Mondo[2] · Igor V. Grigoriev[2,3] · Eric M. Young[1]

Received: 22 July 2024 / Revised: 4 December 2024 / Accepted: 6 December 2024

Abstract

Transcriptomics is a powerful approach for functional genomics and systems biology, yet it can also be used for genetic part discovery. Here, we derive constitutive and light-regulated promoters directly from transcriptomics data of the basidiomycete red yeast *Xanthophyllomyces dendrorhous* CBS 6938 (anamorph *Phaffia rhodozyma*) and use these promoters with other genetic elements to create a modular synthetic biology parts collection for this organism. *X. dendrorhous* is currently the sole biotechnologically relevant yeast in the *Tremellomycete* class—it produces large amounts of astaxanthin, especially under oxidative stress and exposure to light. Thus, we performed transcriptomics on *X. dendrorhous* under different wavelengths of light (red, green, blue, and ultraviolet) and oxidative stress. Differential gene expression analysis (DGE) revealed that terpenoid biosynthesis was primarily upregulated by light through *crtI*, while oxidative stress upregulated several genes in the pathway. Further gene ontology (GO) analysis revealed a complex survival response to ultraviolet (UV) where *X. dendrorhous* upregulates aromatic amino acid and tetraterpenoid biosynthesis and downregulates central carbon metabolism and respiration. The DGE data was also used to identify 26 constitutive and regulated genes, and then, putative promoters for each of the 26 genes were derived from the genome. Simultaneously, a modular cloning system for *X. dendrorhous* was developed, including integration sites, terminators, selection markers, and reporters. Each of the 26 putative promoters were integrated into the genome and characterized by luciferase assay in the dark and under UV light. The putative constitutive promoters were constitutive in the synthetic genetic context, but so were many of the putative regulated promoters. Notably, one putative promoter, derived from a hypothetical gene, showed ninefold activation upon UV exposure. Thus, this study reveals metabolic pathway regulation and develops a genetic parts collection for *X. dendrorhous* from transcriptomic data. Therefore, this study demonstrates that combining systems biology and synthetic biology into an omics-to-parts workflow can simultaneously provide useful biological insight and genetic tools for nonconventional microbes, particularly those without a related model organism. This approach can enhance current efforts to engineer diverse microbes.

Key points

- *Transcriptomics revealed further insights into the photobiology of X. dendrorhous, specifically metabolic nodes that are transcriptionally regulated by light.*
- *A modular genetic part collection was developed, including 26 constitutive and regulated promoters derived from the transcriptomics of X. dendrorhous.*
- *Omics-to-parts can be applied to nonconventional microbes for rapid "onboarding".*

Keywords *X. dendrorhous* · Nonconventional yeast · Transcriptomics · Genetic parts · Photobiology

Introduction

Yeasts are a diverse group of fungi characterized by unicellular growth, which is useful in industrial fermentations. The group is not monophyletic, rather the yeast state has emerged several times across the fungal kingdom (Nagy et al. 2014). Therefore, yeasts have different genome architectures,

Emma E. Tobin and Joseph H. Collins contributed equally.

Extended author information available on the last page of the article

Published online: 28 December 2024

metabolic capabilities, and stress tolerances that are not only due to the ecological niches to which they are adapted, but also due to their different lineages (Boekhout et al. 2022). The impact this biodiversity might have on synthetic biology and industrial biotechnology is currently being explored (Steensels and Verstrepen 2014; Wagner and Alper 2016). However, the different lineages limit the transferability of genetic tools between yeasts (Zeevi et al. 2014), particularly for the basidiomycete yeasts that are not closely related to any model organism (Otoupal et al. 2019). Genomics analysis of the fungal kingdom is well-developed (Libkind et al. 2020; Peris et al. 2023; Merényi et al. 2023), which is a foundation that could be leveraged to derive a collection of genetic parts in addition to enabling insight into fundamental biology.

The model yeast, the ascomycete *Saccharomyces cerevisiae*, has long been the host of choice for yeast metabolic engineering (Da Silva and Srikrishnan 2012; Hong and Nielsen 2012; Galanie et al. 2015; Young et al. 2018). While valuable for converting hexoses to ethanol, engineering *S. cerevisiae* to consume other carbon sources and produce other economically valuable compounds can require extensive reprograming, which imposes metabolic and gene expression burden (Karim et al. 2013; Li et al. 2022). This limitation has led to a growing body of literature that investigates other yeasts, termed nonconventional simply because they are not *S. cerevisiae*, as potential hosts for metabolic engineering since they are already adapted to consume desired carbon sources, produce desired classes of molecules, and tolerate different fermentation conditions; thus, less burden is incurred when engineering them (Yaguchi et al. 2017; Löbs et al. 2017).

Despite their promise, developing genomics and genetic tools in nonconventional yeasts is challenging. This is because a high-quality genome, gene regulatory data, genetic parts and tools for genome engineering, and efficient transformation procedures are often missing. The process of developing these elements, termed "onboarding," can be accelerated for nonconventional ascomycete yeasts closely related to *S. cerevisiae* because the genomics and genetics are similar, permitting transfer of similar promoter and plasmid designs (Durmusoglu et al. 2023). Onboarding organisms from relatively unknown classes, particularly basidiomycete yeasts, does not have this advantage because there is not a closely related model organism.

Xanthophyllomyces dendrorhous is a nonconventional yeast that has gained attention in the aquaculture (Storebakken et al. 2004) and nutraceutical (Ambati et al. 2014) industries due to its natural ability to produce astaxanthin, a vibrant red pigment with potent antioxidant properties (Naguib 2000). Because of its industrial potential, *X. dendrorhous* research has been centered around response to stressors (Santopietro et al. 1998), ability to utilize low-cost carbon sources (Gervasi et al. 2018; Lai et al. 2023), mutagenesis (Gassel et al. 2013), astaxanthin extraction techniques (Mussagy et al. 2022), and characterization of carotenogenic-adjacent pathways and enzymes (An et al. 1999). Several studies have reported genetic engineering of *X. dendrorhous*, including knock-out of genes (Loto et al. 2012) and increasing gene copy number (Breitenbach et al. 2011; Ledetzky et al. 2014).

A high-quality genome sequence, a modular gene expression parts collection, and efficient transformation methods are needed for a nonconventional organism to become a host for high-throughput genome engineering. To that end, successful transformation of *X. dendrorhous* was first reported in 1997 (Wery et al. 1997). Yet, while *X. dendrorhous* currently has several genomes sequenced (Sharma et al. 2015; Bellora et al. 2016), these lack the chromosomal resolution that can now be achieved with modern hybrid resequencing methods that combine short and long reads (Collins et al. 2021). Additionally, *X. dendrorhous* lacks a modular gene expression part collection. So far, only 8 constitutive promoters from central carbon metabolism are available (Rodríguez-Sáiz et al. 2009; Hara et al. 2014). Furthermore, complex but uncharacterized regulation of the astaxanthin biosynthetic pathway limits utilization of this organism as a platform for production (Tropea et al. 2013; Stachowiak 2013; Huang et al. 2022; Li et al. 2023). Therefore, a combined genomics and transcriptomics effort could reveal the key regulatory targets for metabolic engineering and yield additional promoters for high-throughput genome engineering.

Here, we describe an omics-driven workflow from genome sequencing and transcriptomics to a modular gene expression parts collection for *X. dendrorhous*. The transcriptomics data generated allows insights into the genetic basis of how light affects carotenogenic gene expression and utilizes this new understanding to develop a modular parts library in *X. dendrorhous.* The final parts collection contains 26 promoters within a hierarchical "GoldenGate" Type IIS enzyme assembly strategy that includes terminators, selection markers, reporters, and integration cassettes. Therefore, this combined systems and synthetic biology approach delivers insight, parts, and tools for a nonconventional yeast without a closely related model.

Material and methods

Strains and media

The *X. dendrorhous* type strain CBS 6938 (ATCC 96594) was cultured at 21 °C in YPD (YEP, Sunrise Science, Knoxville, TN, USA, 1877-1 KG) plus 20 g/L glucose, Alfa Aesar, Haverhill, MA, USA, A16828) media for all experiments. For all light plate apparatus experiments, the *X. dendrorhous* seed cultures were shielded from any external light by wrapping

the flasks with aluminum foil. *X. dendrorhou*s transformants were selected using YPD with 30 mg/L nourseothricin (Jena Bioscience, Jena, Germany, AB-101-10ML). Solid media plates were made using 20 g/L agar (Sunrise Science, Knoxville, TN, USA, 1910-1 KG). Golden gate (Type IIS) cloning was conducted using chemically competent *Escherichia coli* DH5α cells (NEB, Ipswich, MA, USA, C2987H). Construction of destination vectors with the toxic selection marker *ccdB* was done with chemically competent One Shot *ccdB* Survival 2 T1R *E. coli* cells (Invitrogen, Waltham, MA, USA, A10460). Both *E. coli* strains were grown in 25 g/L LB Miller broth (Fisher Scientific, Hampton, NH, USA, BP1426-2) at 37 °C. Antibiotic selection was carried out using 100 mg/L carbenicillin (Alfa Aesar, Haverhill, MA, USA, J61949), 25 mg/L chloramphenicol (Alfa Aesar, Haverhill, MA, USA, B20841), and 50 mg/L kanamycin (Alfa Aesar, Haverhill, MA, USA, J61272) for level 0, level 1, and level 2 assemblies, respectively.

gDNA isolation and sequencing

Isolation of gDNA from *X. dendrorhous* and next-generation sequencing was performed as described by Collins et al. (2021). Benchmarking universal single-copy ortholog (BUSCO) analyses were conducted on nine publicly available *X. dendrorhous* genomes using basidiomycota_odb10 for a lineage, Augustus 3.2 for gene prediction, and *Ustilago maydis* as the Augustus species (Stanke et al. 2006; Manni et al. 2021a, b; Manni et al. 2021a, b). Genomes were sourced from GenBank (https://www.ncbi.nlm.nih.gov/genbank/) and assembly identifiers were as follows; GCA_001007165.2 (Sharma et al. 2015), GCA_001600435.1 (RIKEN Center for Life Science Technologies, Wako, Japan 2016), GCA_001579715.1 (Bellora et al. 2016), GCA_014706385.1 (Gómez et al. 2020), GCA_019201825.1 (Xiamen Canco Biotech Co., Fujian, China 2021), GCA_023566135.1 (Nanjing Tech University, Nanjing, China 2022), GCA_028533015.1 (Luna-Flores et al. 2022), GCA_022059005.1 (Jilin Agricultural University 2022), and GCA_037127225.1 (this study).

Construction of a light plate apparatus for various light wavelengths

The light plate apparatus (LPA) was assembled following a user's manual published by the Tabor lab at Rice University (Gerhardt et al. 2016). The LPA is an instrument capable of shining two individual LED lights on cell cultures in a 24-well plate. It is comprised of a 3D-printed shell surrounding a soldering board with 48 LED light sockets oriented below a 24-well plate with a clear bottom (Arctic White LLC, Lehigh Valley, PA, USA, AWLS-324042). The LPA allows each culture to be exposed to two unique LED lights without disrupting neighboring cultures.

RNA isolation from the light plate apparatus

LPA cultures were started in 2 mL of YPD media at $OD_{600} = 1$ and shaken for 4 h at 200 rpm while exposed to one red ($\lambda = 660$ nm), green ($\lambda = 565$ nm), blue ($\lambda = 470$ nm), white (visible light spectrum), or UV LED light ($\lambda = 400$ nm), or no LED light. For the transcriptome sequencing experiments, the hydrogen peroxide condition replaced the white light condition. The hydrogen peroxide condition consisted of YPD media with hydrogen peroxide at a concentration of 10 mM and had no LED light. Then, 1 mL of *X. dendrorhous* culture was taken forward for RNA isolation, which used a cell homogenization and TRIzol-based method. *X. dendrorhous* cells were first resuspended in 200 µL of cell lysis buffer (0.5 M sodium acetate, 5% sodium dodecyl sulfate (SDS), and 1 mM ethylenediaminetetraacetic acid (EDTA)) and transferred to pre-filled tubes with 400-micron zirconium beads (OPS diagnostics, Lebanon, NJ, USA, PFMB 400–100-34). The cells were homogenized using a FastPrep-24 machine from MP Biomedical, Irvine, CA, USA, for two cycles at 6 m/s for 30 s each, with a 1-min incubation on ice between each cycle. Then, 800 µL of TRIzol reagent (Invitrogen, Waltham, MA, USA, 15,596,026) was then added to the cell lysate and incubated on ice for 10 min, followed by two more cycles on the FastPrep machine. On ice, 100 µL of 1–bromo–3–chloropropane (Sigma Aldrich, Burlington, MA, USA, B9673-200ML) was added to the cell lysate, inverted to mix, and incubated for 5 min. The tubes were spun down at 4 °C for 14,000 × g for 15 min. Then, 400 µL of supernatant was transferred to 400 µL of 100% ethanol. The RNA was purified using the Monarch Total RNA Miniprep Kit (NEB, Ipswich, MA, USA, T2010S) following the supplier's instructions.

qRT-PCR evaluation of carotenogenesis pathway activity in response to light exposure

RNA samples were converted to cDNA using the Protoscript II First-Strand cDNA Synthesis Kit (NEB, Ipswich, MA, USA, E6560S) following the supplier's standard protocol instructions. RT-qPCR was then performed using IDT's PrimeTime Gene Expression Master Mix (Integrated DNA Technologies Inc., Coralville, IA, USA, 1,055,772) and PrimeTime qPCR pre-mixed assay with probes and primers. Sequences can be found in Supplemental Table S1. Probes targeting genes-of-interest were labeled with fluorescein amidite (FAM) fluorophores and probes targeting the actin housekeeping gene were labeled with hexachlorofluorescein (HEX) fluorophores. qRT-PCR was performed in triplicate. Primers were designed on Benchling (https://benchling.com/) and optimal probe placement was determined using PrimerQuest (https://www.idtdna.com/PrimerQuest). The QuantStudio 6 Flex system (Applied Biosystems, Waltham,

MA, USA, 4,485,699) was used, and instructions provided by Integrated DNA Technologies for the standard cycling protocol were followed. qRT-PCR bar graphs were generated using GraphPad Software, Boston, MA, USA (www.graphpad.com).

RNA transcriptome sequencing and differential gene expression analysis

cDNA preparation and sequencing were performed per JGI's standard workflow. Raw FASTQ file reads were filtered and trimmed using the Joint Genome Institute (JGI) QC pipeline (Clum et al. 2021). Filtered reads from each library were aligned to the reference genome using HISAT version 0.1.4-beta (Kim et al. 2015). featureCounts (Liao et al. 2014) was used to generate the raw gene counts file using gff3 annotation. Raw gene counts were used to evaluate the level of correlation between biological replicates using Pearson's correlation (Benesty et al. 2009) and determine which replicates would be used in the differential gene expression (DGE) analysis. DESeq2 (version 1.10.0) was subsequently used to determine which genes were differentially expressed between pairs of conditions (Love et al. 2014). The parameter used to call a gene differentially expressed between conditions was a p-value < 0.05. Three biological replicates were performed for each treatment. Promoter names were determined by comparing gene annotations across ERGO's gene ontology, Interpro, JGI predictions, and BLAST results, as shown in Supplemental Table S2. Heatmaps were generated through GraphPad Software, Boston, MA, USA (www.graphpad.com) and Adobe Illustrator (https://adobe.com/products/illustrator). Microsoft Powerpoint (https://office.microsoft.com/powerpoint) was used to generate protocol figures.

Gene set enrichment analysis

Annotated *X. dendrorhous* CBS 6938 genome and gene count table from mapped transcriptomic reads were uploaded to ERGO 2.04 (Igenbio, Chicago, IL, USA) (Overbeek 2003). Genes were functionally enriched according to ERGO groups using GAGE5 (Luo et al. 2009).

Polymerase chain reaction (PCR)

All PCRs were done using Q5 2X Master Mix (NEB, Ipswich, MA, USA, M0492L). Primers were designed on Benchling (https://benchling.com/). The OligoAnalyzer tool from Integrated DNA Technologies (IDT) (https://www.idtdna.com/pages/tools/oligoanalyzer) and the NEB T_m Calculator (https://tmcalculator.neb.com/) were used to check primer features. All primers were ordered from Integrated DNA Technologies, Coralville, IA, USA. PCR reactions closely followed NEB instructions. Briefly, reactions were done in 50 µL total volume; 25 µL Q5 Master Mix, 2.5 µL of each primer, X µL of template DNA (1 ng plasmid DNA or 100 ng genomic DNA), and 20-X µL nuclease free water (VWR, Radnor, PA, USA, 02–0201-0500). Reactions were run on a thermocycler following the manufacturer instructions.

Gibson cloning

Gibson assembly was used to construct destination vectors, which were designed for Type IIS-based cloning. Benchling (https://benchling.com/) was used to simulate Gibson assemblies. Reactions closely followed instructions from the NEBuilder HiFi DNA Assembly Master Mix (NEB, Ipswich, MA, USA, E2621S). Fragments were amplified with PCR and designed to have 20–30-bp overlaps. The *Dpn*I enzyme was used to digest template plasmid or *X. dendrorhous* genomic DNA according to the manufacturer's instructions (NEB, Ipswich, MA, USA, R0176S). Calculations and conversions were performed with aid of NEBioCalculator (https://nebiocalculator.neb.com). The amplified fragments were purified using the Zymo Clean and Concentrator Kit (Zymo, Irvine, CA, USA, D4005), followed by dilution to 0.2 pmols for 2–3 fragments or 0.5 pmols for 4 or more fragments. The fragments, 10 µL of HiFi master mix, and nuclease free water were combined in a PCR tube for a 20-µL total reaction volume. The mixture was run on a thermocycler at 50 °C for 60 min, with a hold at 10 °C.

Type IIS cloning and parts

A modular, hierarchical Type IIS cloning scheme was used to construct genetic designs for integration into *X. dendrorhous* (Iverson et al. 2016). This scheme consisted of three levels: transcriptional parts (level 0), transcription units (level 1), and integrative pathways (level 2). Cloning reactions were based on the enzymes *Bbs*I (Thermo Scientific, Waltham, MA, USA, ER1011) or *Bsa*I (NEB, Ipswich, MA, USA, R3733). Benchling (https://benchling.com/) was used to simulate Type IIS reactions. Cloning reactions consisted of 1 µL of N parts, 1 µL of *Bsa*I or *Bbs*I, 1 µ L of 10X Ligase Buffer, 0.4 µL of T4 DNA ligase (Promega, Madison, WI, USA, M1794), and 7.9 – N µL of nuclease free water, where N is the number of parts. Reactions were run on a thermocycler at 37 °C for 5 h, 50 °C for 15 min, 80 °C for 20 min, and a hold at 10 °C. All genetic parts used in this study can be found in Supplemental Table S3. All cloning vector maps can be found in Supplemental Fig. S1.

Minimum inhibitory concentration assay

X. dendrorhous cultures were diluted with YPD to an $OD_{600} = 1.0$ and 100 µL was pipetted into columns 2–11 of a 96-well plate (Corning, Corning, NY, USA, 3596). Column 11 served as a positive control of only *X. dendrorhous* culture. A negative control of 100 µL YPD was pipetted into column 12. The antifungals hygromycin (ThermoFisher, Waltham, MA, USA, 10,687,010), zeocin (Jena Bioscience, Jena, Germany, AB-103S), geneticin (ThermoFisher, Waltham, MA, USA, 10,131–035), and nourseothricin (Jena Bioscience, Jena, Germany, AB-101L) were chosen for the experiment. Stocks of each antifungal were made in concentrations of 5120 µg/mL and 7680 µg/mL. Five biological replicates of antifungal concentration were made by pipetting 200 µL of an antifungal into three wells of column 1. A multichannel pipette was used to perform a serial dilution to column 10. At column 10, 100 µL of the culture and antibiotic mixture was pipetted and discarded, leaving 100 µL of mixture in every well. The 96-well plates were incubated at 21 °C for 3 days. The OD_{600} was measured using Biotek's Gen 5 software on a BioTek Synergy H1 plate reader (Agilent, Lexington, MA, USA, SH1FSN) with column 12 as a blank. Survival percentage was calculated by the following equation: $\frac{OD_{600}A}{OD_{600}PC} \bullet 100\%$ where OD_{600}A represents the average OD_{600} associated with a certain antibiotic concentration and OD_{600}PC represents the average OD_{600} for the positive controls in column 11. Outliers were calculated using an interquartile range and were excluded in survival percent calculations. Outliers were distributed nearly evenly across all four antibiotics treatments with 16 in the hygromycin data, 13 in the nourseothricin data, 15 in the zeocin data, and 20 in the geneticin data. Outliers were calculated and removed due to imperfect measurements of plate readers with heavy yeast cells, such as *X. dendrorhous*. Data calculations and figures were made with Microsoft Excel (https://office.microsoft.com/excel).

X. dendrorhous transformation

Integrative pathway DNA for transformation was excised from level 2 vectors with a *Bsa*I digestion. This digestion was comprised of 40 µL plasmid DNA, 5 µL 10X CutSmart Buffer, 2 µL *Bsa*I, and 3 µL nuclease free water. The reaction was run at 37 °C for 10 h, 80 °C for 20 min, and a hold at 10 °C. The resulting DNA fragments were then purified with the Zymo Clean and Concentrator Kit (Zymo, Irvine, CA, USA, D4004) and were ready for transformation. *X. dendrorhous* transformations were based on an electroporation method described by Visser et al. (2005). *X. dendrorhous* was first streaked on a YPD agar plate and grown at 21 °C for approximately 2 days. A single colony was used to inoculate 50-mL YPD media in a 125-mL Erlenmeyer flask. The cells were shaken at 21 °C and 200 rpm for another 2 days. These cells were then used to inoculate 200 mL of YPD in a 1-L Erlenmeyer flask at $OD_{600} = 0.02$. The cells were grown at 21 °C and 200 rpm until reaching $OD_{600} = 1.2$ (approximately 20 h). From here, the cells were pelleted at 1500 × g for 5 min and resuspended in 25 mL of freshly made 50 mM potassium phosphate buffer (pH = 7.0, Sigma Aldrich, Burlington, MA, USA, P8281-100G and P9791-100G) with 25 mM diothiothreitol (Acros Organics, Geel, Belgium, 426,380,500). The cells were incubated at room temperature for 15 min and then pelleted at 4 °C for 5 min at 1500 × g. The cells were then washed with 25 mL of ice cold STM buffer (pH = 7.5, 270 mM sucrose, Millipore Sigma, Burlington, MA, USA, 1.07651.5000, 10 mM Tris HCl, Alfa Aesar, Haverhill, MA, USA, J67233, 1 mM $MgCl_2$, VWR, Radnor, PA, USA, E525-100ML) and spun down again at 4 °C for 5 min at 1500 × g. This wash step was repeated and followed by resuspension of the pellet in 500 µL of STM buffer. Now electrocompetent, the cells were divided into 60 µL aliquots and kept on ice until electroporation. Then, 10 µL of transforming DNA was mixed with a 60 µL aliquot and transferred to an ice cold 0.2-cm electroporation cuvette (ThermoFisher, Waltham, MA, USA, 21–237-2). Electroporation was performed with a Gene Pulser electroporator (Bio-Rad, Hercules, CA, USA, 1998.018.1, 1998.018.2, and 1998.018.3) at 0.8 kV, 1000 Ohms, and 25 µF. Immediately following the electric pulse, 500 µL of ice cold YPD was added to the cuvette. This mixture was then transferred to 4 mL of YPD in a 14-mL Falcon tube and grown overnight on a rotating drum. The next morning, the cells were spun down for 5 min at 1500 × g, resuspended in 500 mL of filtered water, and spread onto selection plates. The plates were incubated at 21 °C until colonies appeared, which typically occurred in 2–3 days. All strain modifications performed on CBS 6938 can be found in Supplemental Table S4. Microsoft PowerPoint (https://office.microsoft.com/powerpoint) was used to generate protocol figures.

Astaxanthin extraction from wild-type and crtYB knockouts

X. dendrorhous CBS 6938 wild-type and *crtYB* knockout strains were grown for 3 days in the dark at 21 °C and 200 rpm. Then, 1 mL of culture was taken forward and centrifuged at 10,850 × g for 10 min. The cell pellet was washed with Milli-Q filtered water twice before resuspension in 1 mL of acetone (Sigma Aldrich, Burlington, MA, USA, 34,850-1L). Cell and acetone mixtures were poured into pre-filled tubes of 400-micron zirconium beads (OPS Diagnostics, Lebanon, NJ, USA, PFMB 400–100-34) and then transferred to snap-cap microcentrifuge tubes

(Eppendorf, Framingham, MA, USA, 022363743). The Bullet Blender Storm Pro tissue homogenizer (NextAdvance, Troy, NY, USA, BT24M) was used at 12 m/s for 5 min to mechanically lyse the cells. Afterward, tubes were centrifuged for 10,850 × g for 10 min. Then, 200 µL of supernatant was pipetted into a nylon syringeless filter (Cytiva, Marlborough, MA, USA, UN203NPENYL) and transferred to a 2-mL chromatography vial (Agilent, Lexington, MA, USA, 5181–3376) with a glass vial insert (5183–2085) and crimp top cap (Agilent, Lexington, MA, USA, 8010–0051).

Chromatography (UPLC) detection of astaxanthin

Ultra-performance liquid chromatography (UPLC) analysis was performed using a modified method from Bohoyo-Gil et al. (2012). Modifications include an injection volume of 10 µL, usage of a Shimadzu Nexcol C18 column (1.8 µm, 50 mm × 2.1 mm) (Shimadzu, Columbia, MD, USA, 220–91394-03), and analysis on the Nexera Series UPLC (Shimadzu, Columbia, MD, USA; RF-20AXS, RID-20A, SCL-40, DGU-403, DGU-405, CTO-40C, SPD-M40, C-40 LPGE, LC-40D XS, SIL-40C XS). The flow rate was 0.3 mL/min and a gradient method was performed. The mobile phase consisted of water treated formic acid (0.1%) (A) acetonitrile (B), ethyl acetate (C), and methanol (D). The gradient followed: 0.00–4.00 min, 85% A and 15% C; 4.00–4.01 min, 60% A, 20% B, and 20% C with a hold until 9 min; and 9.00–9.01 min, 85% A, 15% D with a hold until 10 min. The UV–vis spectra were recorded between 190 and 600 nm. Peaks were detected at 460 nm. The column temperature was maintained at 28 °C. Sample temperatures were maintained at 4 °C. The retention time of astaxanthin was 0.96 ± 0.02. The Shimadzu LabSolutions software (https://www.ssi.shimadzu.com/products/software-informatics/labsolutions-series/labsolutions-cs) and Microsoft Excel (https://office.microsoft.com/excel) were used for analysis. Adobe Illustrator (https://adobe.com/products/illustrator) was used to edit chromatograms.

Bioluminescence detection assay

LPA cultures were started in 2 mL of YPD media at $OD_{600} = 1$ and shaken for 24 h at 200 rpm. *X. dendrorhous* was exposed to either a UV ($\lambda = 400$ nm) or dark (no LED light) condition. Bioluminescence was detected using the Nano-Glo Luciferase Assay System (Promega, Madison, WI, USA, N1110). Assay buffer and assay reagent were mixed in a 50: 1 ratio to create to assay solution. Aliquots of 50 µL of *X. dendrorhous* cells were mixed with 50 µL assay solution in a 96-well plate (Corning, Corning, NY, USA, 3904). Bioluminescence was measured on a BioTek Synergy H1 plate reader (Agilent, Lexington, MA, USA, SH1FSN) with Biotek's Gen 5 Software for Imaging and Microscopy (https://www.agilent.com/en/product/cell-analysis/cell-imaging-microscopy/cell-imaging-microscopy-software/biotek-gen5-software-for-imaging-microscopy-1623226). Microsoft Excel (https://office.microsoft.com/excel) was used to generate figures.

Results

High-quality contiguous genome of *X. dendrorhous* CBS 6938

A high-quality *X. dendrorhous* CBS 6938 genome was obtained through our previously reported workflow (Collins et al. 2021). The resulting resequenced genome consists of sixteen contigs over 100-kb long, and relative lengths of the contigs are depicted in Supplemental Fig. S2a. We compared this genome to eight publicly available genomes (Supplemental Table S5). Comparatively, the genome obtained in this study has the second least number of contigs overall and contigs over 100-kb long while maintaining a large ungapped genome size of 19.5 Mb. The only genome that outperforms these genome statistics is that of Gómez et al. [2020]. However, subsequent benchmarking universal single-copy ortholog (BUSCO) analysis revealed that the resequenced CBS 6938 genome reported here contains 76.7% complete and single-copy BUSCOs, which is marginally greater than most publicly available genomes, including that reported by Gómez et al. [2020] (Supplemental Fig. S2b).

Foundational genetic tools for onboarding *X. dendrorhous*

In addition to obtaining an accurate genome sequence, we performed a set of experiments to make *X. dendrorhous* easier to engineer. We first examined available selection agents. Rather than seek to create synthetic auxotrophy, which has a variety of metabolic impacts (Mülleder et al. 2012), we screened for antibiotic sensitivity to geneticin, hygromycin, nourseothricin, and zeocin (Wery et al. 1997; Gassel et al. 2013; Yamamoto et al. 2016). The results of the minimum inhibitory concentration (MIC) assay ("Material and methods") are shown in Fig. 1a. The most effective compound was found to be nourseothricin with 11.6% cell survival at a concentration of 10 µg/mL. Thus, we synthesized a *X. dendrorhous* codon optimized version of the *natR* gene for selection in subsequent engineering, termed *XdNatR* (sequence in Supplemental Table S3).

We then designed a modular cloning system for rapidly assembling *X. dendrorhous* genetic elements (Fig. 1b). This system uses the same enzymes and scars as previously published modular cloning systems based on Type IIS restriction enzymes, often termed GoldenGate assembly (Iverson et al. 2016; Young et al. 2018). Like those systems, the *X. dendrorhous* system consists of level 0 genetic elements

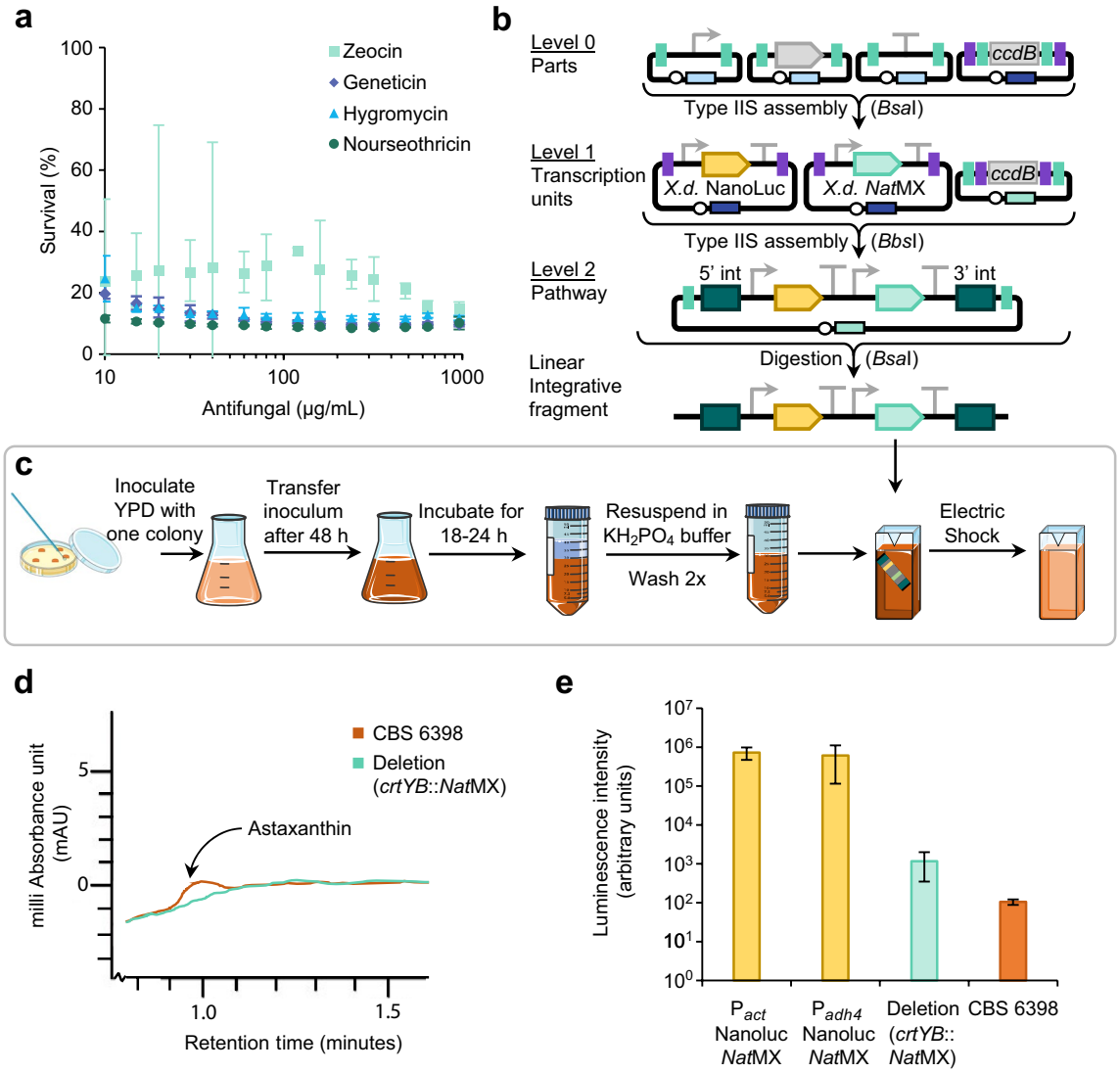

Fig. 1 Improving foundational *X. dendrorhous* genetic tools. **a** Minimum inhibitory concentration (MIC) results depicting the survival percentage of *X. dendrorhous* CBS 6938 when exposed to the antibiotics zeocin, geneticin, hygromycin, and nourseothricin. **b** Hierarchical Type IIS enzyme assembly strategy to generate fragments for homologous recombination into the *crtYB* site. **c** Servier Medical Art (https://creativecommons.org/licenses/by/4.0/) depiction of the high-efficiency transformation procedure. **d** Confirmation of deletion of *crtYB* activity via UPLC. Wild-type is shown in red and the *crtYB* knockout is shown in black. Overlapped UPLC chromatograms show the lack of astaxanthin at a retention time of 0.998 min in the strain with the *XdNat*MX cassette inserted. **e** Luminescence (arbitrary units) of two strains expressing Nanoluc with strong constitutive promoters, P_{act} and P_{adh4}, the *X. dendrorhous crtYB*::*NatMX* deletion, and the *X. dendrorhous* CBS 6938 wild type. Abbreviations for genes: Nanoluc: nanoluciferase; *Nat*MX: nourseothricin resistance transcription unit

(individual promoters, genes, and terminators), level 1 transcription units (combinations of promoters, genes, and terminators), and level 2 integrative plasmids that have homology arms and the ability to integrate several transcription units along with a selection marker (Supplemental Fig. S1). Yet, there are two significant differences. The first is that the *lacZ* element in the destination plasmids is replaced with the lethal gene *ccdB* to shift from blue/white screening of correct clones to a system where only correct clones grow on a selection plate (Bernard et al. 1994). The second is that the homology arms for *S. cerevisiae* were replaced with *X. dendrorhous* homology arms flanking the *crtYB* gene derived from the resequenced genome (Supplemental Table S3). Since the *crtYB* gene product catalyzes the first committed step in visibly colorful terpenoid production, replacement of *crtYB* creates a facile red/white screening method for correctly integrated clones.

To optimize the transformation protocol, an integrative element targeting *crtYB* was built using the elements described above. The known glutamate dehydrogenase promoter (P_{gdh}) and the glycerol-3-phosphate dehydrogenase terminator (T_{gpd}) were combined to express *XdNatR*, creating an *XdNat*MX resistance cassette. This was subsequently

cloned into the integrative pJHCcrtYB1000 plasmid and transformed into *X. dendrorhous* CBS 6938. In our hands, the efficiency of the published transformation was low (Wery et al. 1997), so several modifications were made as described in "Material and methods" and shown in Fig. 1c. Ultra-high-performance liquid-chromatography (UPLC) confirmed successful *crtYB* knock-out—astaxanthin peaks were detected in wild-type but not knock-out extractions (Fig. 1d). Thus, with the design of the integration cassette and confirmation of the transformation protocol, efficient and targeted integration of DNA via homologous recombination into the *X. dendrorhous* genome was perfomed.

We then cloned a luminescent reporter, NanoLuc (England et al. 2016), under the control of two of the known strongest promoters, P_{act} and P_{adh4}, into our modular cloning scheme along with XdNatMX (Fig. 1b), integrated it into the genome, and measured expression via luciferase assay (Fig. 1e). NanoLuc-producing cells created approximately 1000-fold greater luminescence compared to the *crtYB* knockout strain, and nearly 10,000-fold greater luminescence compared to the parent strain. The higher luminescence observed from the *crtYB* knockout strain may be attributed to biological autoluminescence, a phenomenon that has been found to be directly related to oxidative stress (Bereta et al. 2021). Together, these experiments defined selections, reporters, and an integration site for a modular parts collection in *X. dendrorhous* CBS 6938.

Gene expression analysis for part derivation and elucidating photobiology

Of the 8 current available promoters for *X. dendrorhous*, only P_{adh4} and P_{act} have high strength (Hara et al. 2014). Therefore, there is a need for more promoters to enable simultaneous expression of multiple genes in this organism. Furthermore, previous work has shown that astaxanthin metabolism is stimulated by oxidative stress and light (Vázquez 2001; Tropea et al. 2013; Stachowiak 2013; Li et al. 2022), and a white collar 2 transcription factor has been discovered in *X. dendrorhous* (Huang et al. 2022), hinting that *X. dendrorhous* may possess stress and light-inducible transcriptional machinery. Transcriptomics, and particularly differential gene expression (DGE) analysis, can identify both constitutive and regulated genes, which could yield promoters with desired regulation patterns. Yet, it remains unclear if the oxidative and light responses are transcriptionally mediated.

Thus, before conducting transcriptomics, we used the genome sequence to design quantitative polymerase chain reaction (qPCR) probes to target genes in the terpenoid (*MVK*, *PMVK*, *MVD*, *IDI*, *FPS*, and *crtE*) and carotenogenic (*crtYB*, *crtI*, and *crtS*) pathways. We compared the expression of these genes in the dark and under ultraviolet light exposure ("Material and methods"). The log2 fold change (light/dark) of each gene in the pathway is depicted in Fig. 2. Upstream genes *MVK*, *PMVK*, *MVD*, *IDI*, *FPS*, and *crtE* exhibited little to no change in expression between dark and ultraviolet conditions. However, the expression of *crtYB*, *crtI*, and *crtS* was upregulated. Notably, the *crtI* gene showed the highest log2 fold change. This indicates that carotenoid biosynthesis is light regulated through transcriptional activation, while the upstream terpenoid pathway to the diterpenoid intermediate, geranylgeranyl pyrophosphate, is unaffected.

Transcriptomics elucidates *X. dendrorhous* photobiology

Once we established that light influenced carotenogenic transcriptional regulation, we designed a transcriptomics experiment to quantify differential gene expression across dark, ultraviolet, blue, green, and red light, with hydrogen peroxide oxidative stress as a control (Fig. 3a). To perform the experiment, we constructed a Light Plate Apparatus (LPA) to culture *X. dendrorhous* under a variety of conditions (Gerhardt et al. 2016). Sequencing of the samples was done by the Department of Energy Joint Genome Institute, through their Community Science Program, and log2 fold-change in Fragments Per Kilobase of transcript per Million (FPKM) was calculated relative to gene expression in the dark using DESeq2 ("Material and methods").

The impact of light and oxidative stress on the gene expression of several key cellular processes is shown in Fig. 3. This includes the terpenoid and carotenoid pathway (Fig. 3b), putative photoreceptor genes (Fig. 3c), and the top differentially expressed genes in UV and oxidative stress (Fig. 3d and e, respectively).

The terpenoid and carotenoid pathway data corroborated our previous evidence that exposure to ultraviolet light leads to upregulated expression of *crtI* with a log2 fold-change of 0.90. This is below the typically accepted significant log2 fold-change of 1.0, yet the other genes in terpenoid and carotenoid metabolism had no significant changes even at a low threshold of log2 fold-change 0.5. In contrast, oxidative stress upregulated genes in both pathways (*MVK*, *PMVK*, *IDI*, *FPS*, *crtYB*, and *crtI*), with *IDI* having the greatest increase (log2 fold-change of 1.79). This finding is significant because *IDI* is a known bottleneck for the mevalonate pathway in other organisms (Shin et al. 2022). Therefore, a deregulated *IDI* could be a target for increasing flux through the terpenoid pathway in *X. dendrorhous*.

The light response systems in *X. dendrorhous* are relatively unknown, save white collar 2 (Huang et al. 2022). However, systems such as cryptochrome, BLUF-domain, rhodopsin, and photolyase are known in other fungi, including the distantly related basidiomycete *U. maydis* (Yu and Fischer 2019; Brych et al. 2021). Therefore, we searched the *X. dendrorhous* CBS 6938 genome with BLAST for putative fungal photoreceptor proteins within the BLUF, rhodopsin, white collar, and cryptochrome families (Fig. 3c). Photoreceptor proteins predicted

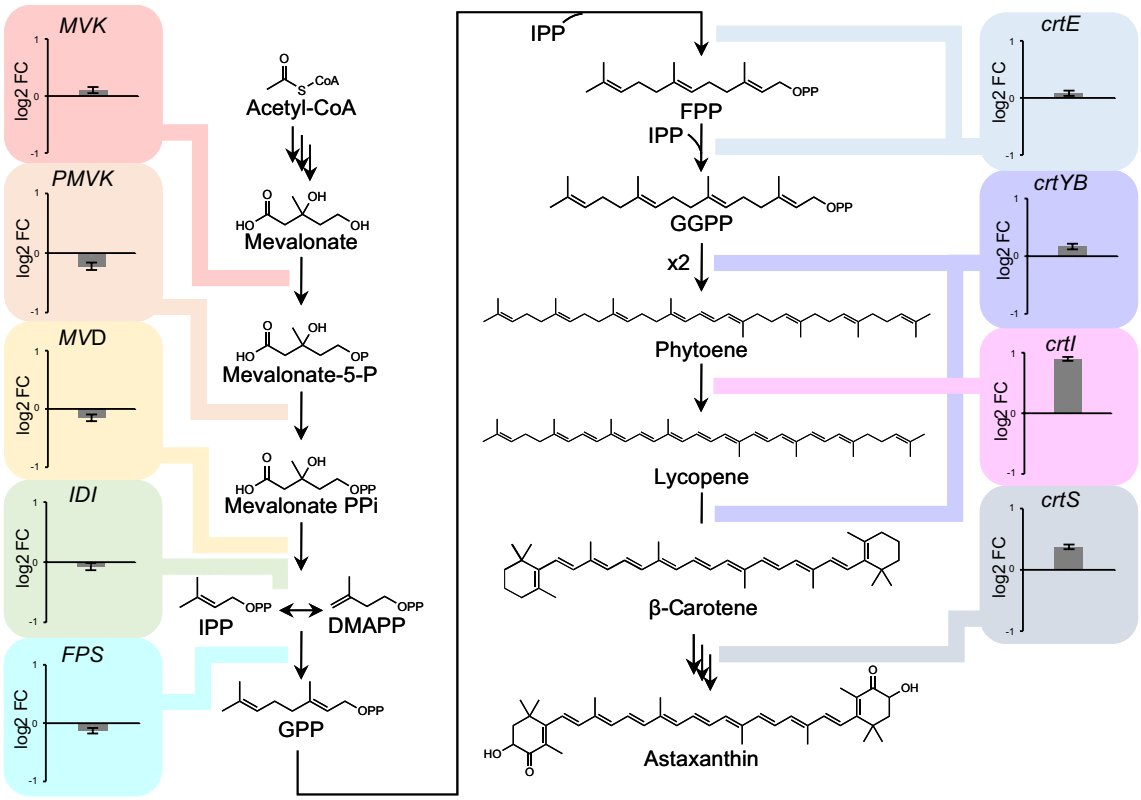

Fig. 2 Transcriptional response of terpenoid and carotenoid biosynthesis in response to ultraviolet light exposure. Differential expression between dark and ultraviolet as measured by the log2 fold change (log2FC) of RT-qPCR ΔΔCt values ("Material and methods"). Upstream mevalonate and terpenoid genes are not affected by ultraviolet, but downstream carotenoid biosynthetic genes *crtI* and *crtS* are upregulated, *crtI* most strongly. Abbreviations for genes: *MVK*: mevalonate kinase; *PMVK*: phosphomevalonate kinase; *MVD*: diphosphomevalonate decarboxylase; *IDI*: isopentenyl-diphosphate isomerase; *FPS*: farnesyl diphosphate synthase; *crtE*: geranylgeranyl pyrophosphate synthase; *crtYB*: bifunctional lycopene cyclase/phytoene synthase; *crtI*: phytoene desaturase; *crtS*: cytochrome-P450 hydroxylase

to be in the same family were differentiated with arbitrarily assigned numbers. We found that the putative cryptochromes increased transcription most dramatically in ultraviolet and blue light exposure. Additionally, putative white collar and rhodopsin genes increased expression. This is evidence that cryptochrome, rhodopsin, and BLUF-domain light response systems exist in *X. dendrorhous*. The oxidative stress condition corroborated that these genes were responding specifically to light because these putative photoreceptors were downregulated or unaffected by hydrogen peroxide.

Finally, we filtered the whole = genome transcriptomic data for the twenty genes with the greatest changes in gene expression under ultraviolet light. Of these twenty, ten upregulated and six downregulated genes had log2 fold-changes of 1.50 or greater (Fig. 3d). Upregulated genes include short-chain dehydrogenase (*SDR*) which is involved in the induction of light-regulated pathways (Bruchez et al. 1996), MSS4-like protein (*MSS4*) which is involved in cell survival through cell cycle regulation and actin cytoskeleton formation (Desrivières et al. 1998), and endonuclease III (*Nth*) which is directly involved in response to ultraviolet stress through DNA repair (Serafini and Schellhorn 1999). These functions collectively correspond to an expected stress response from ultraviolet exposure (Sinha and Häder 2002). Another upregulated gene encoding for conidiation-specific protein 6 (*Con-6*) is involved in the reproductive cycle and is also upregulated after blue-light exposure in *Neurospora crassa* (Olmedo et al. 2010). Unexpectedly, ultraviolet light upregulates expression of glycogenin glucosyltransferase (*GYG*) (Smythe and Cohen 1991; Goldraij and Curtino 1996), an enzyme that initiates glycogen nucleation, and E3 ubiquitin ligase (*E3*), which is involved in growth and protein turnover (Cao and Xue 2021). Also of note, four of the ten upregulated genes were predicted to result in hypothetical proteins, indicating that our understanding of light response mechanisms is incomplete. Several downregulated genes in ultraviolet are involved in the cytochrome c system, including cytochrome c (*CYC1*) itself, cytochrome c peroxidase (*CCP*) (Pelletier and Kraut 1992), and the heme activator protein (*HAP3*) involved in cytochrome c regulation (Hahn and Guarente 1988). Others are mitochondrial electron-transferring-flavoprotein dehydrogenase (*ETFQO*) which is involved in the electron transport

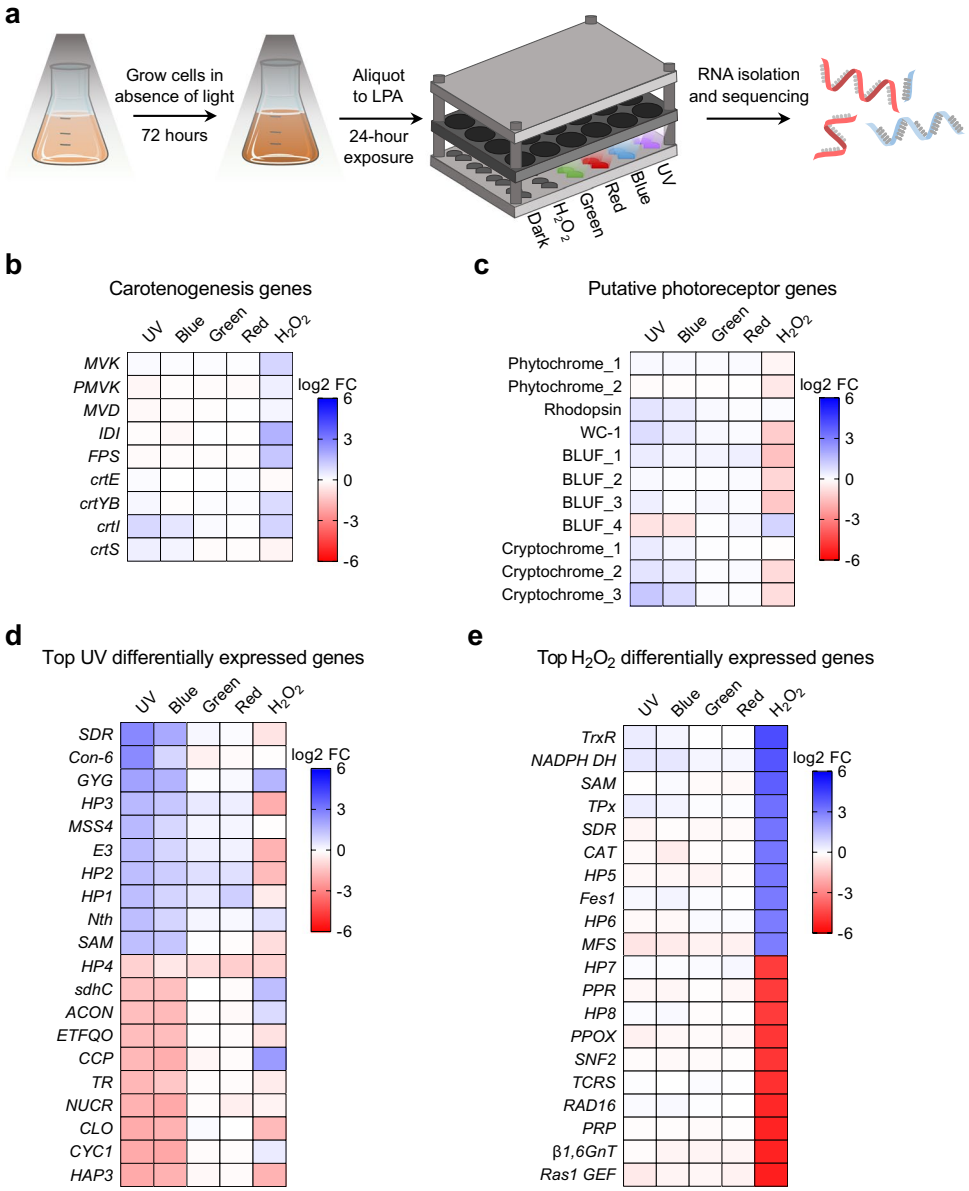

Fig. 3 Transcriptomics and differential gene expression (DGE) of *X. dendrorhous* CBS 6938 under light exposure and oxidative stress. Blue represents induction and red represents repression. Color intensities are equally scaled across charts. **a** Depiction of the experimental workflow for obtaining RNA from *X. dendrorhous* cultured in the light plate apparatus (LPA) under light and hydrogen peroxide stress conditions. **b** Regulation of mevalonate and carotenogenesis genes by light and H_2O_2. Expression of *crtI* and *crtS* is considerably induced by ultraviolet light, and *crtI* is also induced by oxidative stress. **c** Transcriptional response of putative photoreceptor homologs identified by BLAST. The numbers for genes within each class are arbitrarily assigned. **d** Top ten ultraviolet upregulated and downregulated genes. Abbreviations for genes: HP1-4: hypothetical proteins; *SDR*: short-chain dehydrogenase; *Con-6*: conidiation-specific protein 6; *GYG*: glycogenin glucosyltransferase; *MSS4*: phosphatidylinitosol-4-phosphate 5-kinase; *E3*: E3 ubiquitin ligase; *Nth*: endonuclease III; *SAM*: *S*-adenosyl-L-methionine-dependent methyltransferase; *sdhC*: succinate dehydrogenase cytochrome b560 large subunit; *ACON*: aconitate hydratase; *ETFQO*: electron-transferring-flavoprotein dehydrogenase; *CCP*: cytochrome c peroxidase; *TR*: unclassified transcriptional regulator; *NUCR*: unclassified endonuclease; *CLO*: caleosin; *CYC1*: cytochrome c; *HAP3*: transcriptional activator heme activator protein. **e** Top ten H_2O_2-induced and H_2O_2-repressed genes. Abbreviations for genes*: HP5-8*: hypothetical proteins; *TrxR*: thioredoxin reductase; *NADPH DH*: NADPH dehydrogenase; *SAM*: *S*-adenosyl-L-methionine-dependent methyltransferase; *TPx*: thioredoxin reductase; *SDR*: short-chain dehydrogenase; *CAT*: catalase; *Fes1*: Fes1-domain containing protein; *MFS*: major facilitator superfamily permease; *PPR*: pentatricopeptide repeat protein; *PPOX*: protoporphyrinogen oxidase; *SNF2*: SNF2 family DNA-dependent ATPase; *TCRS*: two-component sensor; *RAD16*: DNA repair protein; *PRP*: pre-mRNA-processing-splicing factor; *β1,6GnT*: beta-1,6-*N*-acetylglucosaminyltransferase; *Ras1 GEF*: Ras1 guanine nucleotide exchange factor

chain (Toplak et al. 2019), and caleosin (*CLO*) which is usually upregulated during stress (Rahman et al. 2018), succinate dehydrogenase cytochrome b560 (*sdhC*) (Abraham et al. 1994), and aconitate hydratase (*ACON*) which is an indicator of oxidative stress (Rakhmanova et al. 2023). Two further genes are unclear but labeled as a transcriptional regulator (*TR*) and endonuclease (*NUCR*). We then identified the ten most upregulated and ten most downregulated genes in the hydrogen peroxide exposure condition. Many of these genes are expected and are different from the genes in the light conditions, supporting the idea that light and oxidative stresses elicit separate responses (Fig. 3e).

To more clearly analyze the overall metabolic response to ultraviolet, genes were clustered into functional groups using the ERGO™ Bioinformatics software from Igenbio. Upregulation of functional groups is depicted in Fig. 4a, along with their regulation pattern under oxidative stress. Generally, DNA repair and amino acid metabolic functions were upregulated. Interestingly, aromatic amino acid degradation and modification were upregulated by both ultraviolet

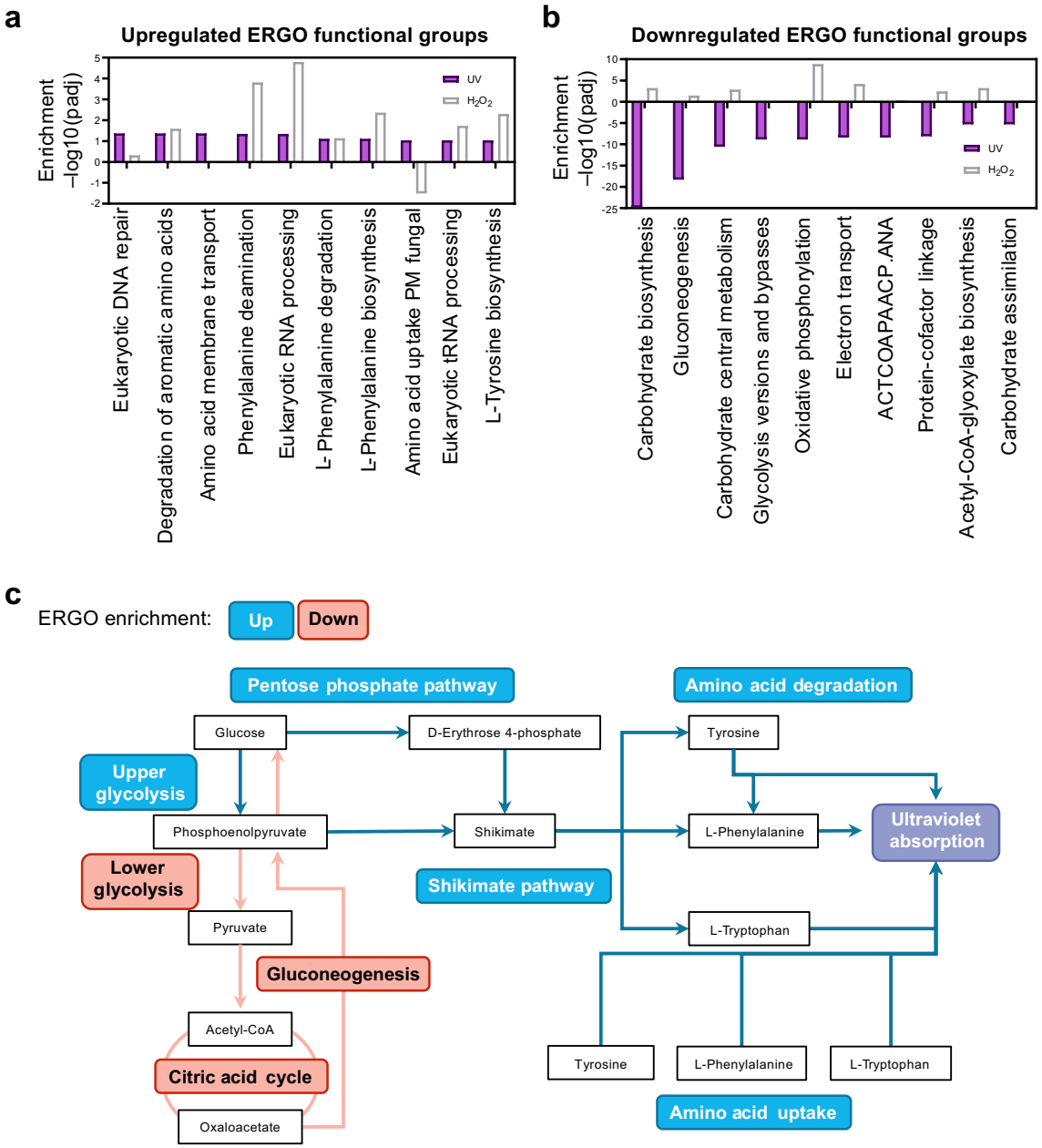

Fig. 4 Transcriptomic analyses clustered by ERGO functional groups. **a** Overall upregulation of metabolic processes by ultraviolet light or H_2O_2. **b** Overall downregulation of metabolic processes by ultraviolet light or H_2O_2. **c** Summary of metabolic processes regulated by ultraviolet light. Generally, metabolic flux is being drawn from central carbon metabolism to synthesis of aromatic amino acids

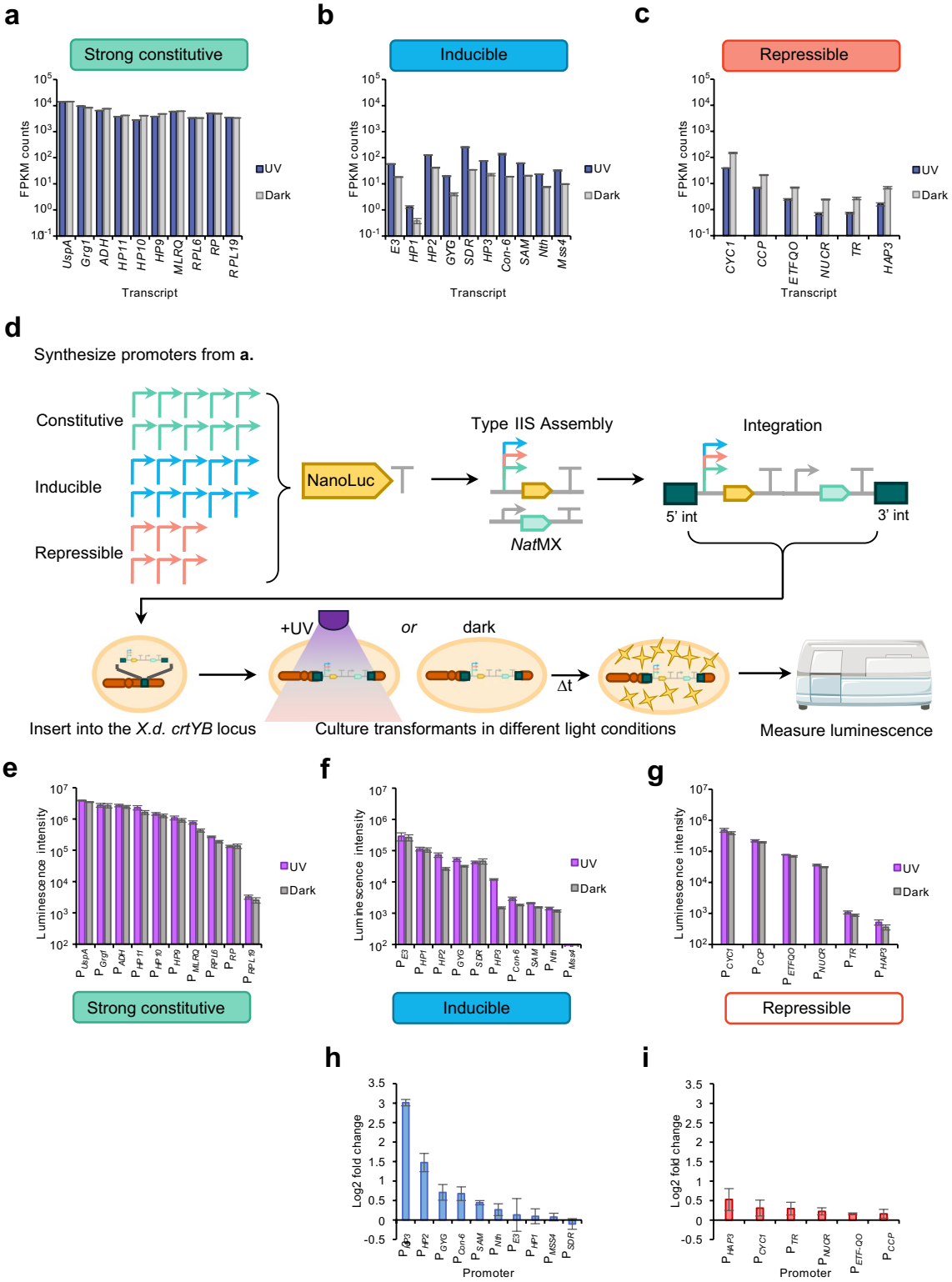

light and hydrogen peroxide, but amino acid uptake was only upregulated in ultraviolet. Furthermore, electron transport, glycolysis, gluconeogenesis, and carbohydrate metabolism were downregulated (Fig. 4b). These results support the general trends observed in the analysis of individual genes described above. Taken together, these observations qualitatively describe a large metabolic shift in response to UV, depicted visually in Fig. 4c. *X. dendrorhous* likely redirects flux from central carbon metabolism to carotenoids and aromatic amino acids upon ultraviolet exposure. Aromatic

◂**Fig. 5** Deriving constitutive and regulated promoters from the transcriptome. **a** FPKM counts of the ten strongest constitutive promoters. Abbreviations for genes: *HP9-11*: hypothetical proteins; *UspA*: universal stress protein A; *Grg1*: glucose-repressible protein 2; *ADH*: alcohol dehydrogenase; *MLRQ*: NADH-ubiquinone reductase complex 1 MLRQ subunit; *RPL6*: ribosomal protein L6P; *RP*: ribosomal protein; *RPL19*: ribosomal protein L19E. **b** FPKM counts of the top 10 inducible promoters, also shown in Fig. 3d. **c** FPKM counts of the top 6 repressible promoters, also shown in Fig. 3d. **d** Hierarchical DNA assembly and expression characterization workflow for each of the 26 promoters. **e** Expression strength of the strong constitutive promoters as measured by Nanoluc luminescence for recombinant *X. dendrorhous* strains grown in the dark or exposed to ultraviolet light. **f** Expression strength of the ultraviolet inducible promoters as measured by Nanoluc luminescence for recombinant *X. dendrorhous* strains grown in the dark or exposed to ultraviolet light. **g** Expression strength of the ultraviolet repressible promoters as measured by Nanoluc luminescence for recombinant *X. dendrorhous* strains grown in the dark or exposed to ultraviolet light. **h** Log2 fold change of luminescence intensity for the inducible promoters. **i** Log2 fold change of luminescence intensity for the repressible promoters

amino acids absorb ultraviolet and are also precursors to other ultraviolet light absorbing molecules like melanin and mycosporine compounds (Gilchrest et al. 1996; Bhatia et al. 2011; Llewellyn et al. 2020). The activation of aromatic amino acid pathways in response to ultraviolet has not been previously observed in basidiomycetes. These results indicate that the response to ultraviolet in *X. dendrorhous* is more extensive and complex than acting on carotenogenesis alone. Furthermore, the significant fraction of hypothetical proteins hints at additional unknown mechanisms that also contribute to the response.

Transcriptomics-driven part selection allows simultaneous derivation of constitutive and regulated genetic parts

We then sought to leverage the DGE data to derive gene expression parts. Since the data covered a variety of conditions, we reasoned that it should be possible to derive putative strong constitutive and regulated promoters. We identified strong constitutive promoters by sorting each transcriptomics dataset by fragments per kilobase of exon per million mapped fragments (FPKM) count, choosing the genes that had the highest and consistent FPKM counts across conditions (Fig. 5a). Notably, the known strong *ADH* promoter is among these, yet no other central carbon metabolism promoters are represented. This result challenges the convention of simply selecting central carbon metabolism promoters as genetic parts for yeasts. Furthermore, the DGE data allowed selection of highly regulated promoters in addition to constitutive. We selected promoters from the 16 genes in Fig. 3d that had log2 fold-changes of 1.50 or greater when exposed to ultraviolet light (Fig. 5b, c, respectively). We used the resequenced genome to obtain the promoter regions upstream of each of these 26 promoters, as defined by a JGI promoter analysis tool. These putative promoters were then cloned into our modular cloning system to drive expression of the luciferase reporter and integrated into the genome (Fig. 5d).

Then, expression of each construct via a luciferase assay in the dark and under ultraviolet exposure was measured ("Material and methods"). As Fig. 5e shows, the constitutive promoters result in high luminescence that does not change between the dark and the light. Many of the putative activated promoters showed increased luminescence in response to ultraviolet (Fig. 5f). However, most of these increases were not large. The two strongest inducible promoters were found to be that of the hypothetical proteins HP3 and HP2 with log2 fold-changes of 3.01 and 1.47, respectively (Fig. 5h). The putative repressed promoters did not show any significant repression (Fig. 5g, i). We reasoned that the long half-life of luciferase was confounding measurement of repression. Thus, we designed a qPCR experiment, and the results indicated no change in transcript levels (data not shown). Therefore, it seems likely that the promoter sequences selected do not contain the regulatory elements, or there could be a variety of context-dependent epigenetic factors.

Taken together, our results show that transcriptomics driven part discovery can consistently derive strong constitutive promoters, but inconsistently derive regulated promoters due to a variety of possible factors. Even so, we were able to discover ten strong promoters as well as two promoters that can be activated by ultraviolet, one of which with ninefold induction under ultraviolet. Thus, our part discovery efforts generated a collection of constitutive and regulated promoters that are compatible with our modular cloning system for *X. dendrorhous* CBS 6938.

Discussion

In this study, a promising nonconventional yeast was subjected to a set of genomics and genetics experiments that transformed it into a host for advanced genetic engineering and synthetic biology. This was done by obtaining a high-quality resequenced genome, developing a modular genetic part collection, analyzing gene regulation, and deriving promoters from transcriptomic data. Now, it is possible to interrogate the unique metabolism and photobiology of *X. dendrorhous* in a similar manner to other nonconventional yeasts.

Our analysis of *X. dendrorhous* photobiology revealed insights into the biological mechanisms of basidiomycete light response. Although previous studies have indicated that light increases astaxanthin production (Vázquez 2001; Stachowiak 2013), we determined that light transcriptionally regulates the carotenoid, or tetraterpenoid, pathway

but not the upstream terpenoid pathway. The key node, *IDI*, is also regulated by the oxidative stress response. We also observed that *X. dendrorhous* engages a variety of survival responses in response to ultraviolet, including activation of DNA repair, activation of reproduction pathways, repression of central carbon metabolism, and repression of mitochondrial respiration. Aromatic amino acid biosynthesis was also upregulated in addition to tetraterpenoid biosynthesis, hinting that the biosynthesis of other light absorbing compounds such as melanins and mycosporines is important in the light response. We also found evidence of multiple different fungal light response systems, including cryptochromes, rhodopsins, and BLUF-domains. Taken together, these data paint a picture of an extensive and coordinated response to light. This complex system is likely key to survival of *X. dendrorhous* in its ecological niche of fallen trees at high altitudes (Libkind et al. 2007), which would include extended periods of intense ultraviolet exposure.

It is interesting to note that our genome integration approach results in efficient on-target insertion of constructs via homologous recombination (HR). Our findings support the results of others that *X. dendrorhous* CBS 6938 has an active HR pathway (Hara et al. 2014), which is beneficial for future strain engineering efforts. This highlights that not all nonconventional yeasts favor the nonhomologous end joining (NHEJ) mechanism (Schwarzhans et al. 2016; Schwartz et al. 2017).

Leveraging transcriptomics was not only key to gaining insight into metabolic regulation, but also enabled selection of constitutive and regulated gene expression parts. Transcriptomics has been previously used to identify regulated promoters in other yeasts (Gasser et al. 2015; Zahrl et al. 2017; Brink et al. 2023). This work builds on this prior evidence, adding a modular cloning standard to create an omics-to-parts workflow that can yield needed constitutive and inducible promoters for construction of genetic devices. It is notable that only one of the ten most transcribed promoters in *X. dendrorhous* was from central carbon metabolism, which challenges the convention that promoters from central carbon metabolism genes are the best choice. Thus, this omics-to-parts workflow may be a more effective route to obtaining genetic parts collections for nonconventional yeasts.

Development of novel production platform hosts requires an understanding of genome composition and genetic regulation, which may also be used for genetic tool and genetic part development. This work demonstrates how an integrated genomics and genetics approach can simultaneously deliver new biological understanding and onboard a nonconventional organism, particularly a nonconventional yeast with no closely related model organism. This integrated approach promises to enhance organism onboarding efforts.

Supplementary Information The online version contains supplementary material available at https://doi.org/10.1007/s00253-024-13379-w.

Author contribution EET, JHC, and EMY conceived of the study. EET and JHC performed all experiments and analysis save the sequencing and initial processing of RNA-seq data. CBM and GTN constructed the light plate apparatus (LPA). KM acquired microscope images of red yeast. AL, SM, and IG performed transcriptomic sequencing and initial processing of RNA-seq data. EET and EMY wrote the manuscript.

Funding This project is supported by a National Science Foundation CAREER award to EMY, award number 1944046. EET is supported by a National Science Foundation Graduate Research Fellowship. The work (proposal https://doi.org/10.46936/10.25585/60001246) conducted by the U.S. Department of Energy Joint Genome Institute (https://ror.org/04xm1d337), a DOE Office of Science User Facility, is supported by the Office of Science of the U.S. The Department of Energy operated under Contract No. DE-AC02-05CH11231. Development of Prymetime genome assembly was supported by the Office of the Director of National Intelligence (ODNI), Intelligence Advanced Research Projects Activity (IARPA) under Finding Engineering Linked Indicators (FELIX) program contract #N66001-18-C-4507.

Data availability The genome was deposited in GenBank under the BioProject PRJNA1053634. Each replicate was registered as an NIH BioSample by JGI and can be found under the accessions SAMN15720006, SAMN15720353, and SAMN15720008 (UV1-3); SAMN15719986, SAMN15719959, and SAMN15720031 (blue1-3); SAMN15720054, SAMN15720004, and SAMN15719987 (green1-3); SAMN15719960, SAMN15719963, and SAMN15720352 (red1-3); SAMN15719962, SAMN15720053, and SAMN15719985 ($H_2O_2$1-3); and SAMN15720005, SAMN15720007, and SAMN15719961 (dark1-3). Additionally, all genomics and transcriptomics data can be found within the JGI genome portal under the JGI Project ID 1255824.

Declarations

Ethics approval This article does not contain any studies with human participants or animals performed by any of the authors.

Disclosure The views and conclusions contained herein are those of the authors and should not be interpreted as necessarily representing the official policies, either expressed or implied, of ODNI, IARPA, or the U.S. Government. The U.S. Government is authorized to reproduce and distribute reprints for governmental purposes notwithstanding any copyright annotation therein.

Conflict of interest The authors declare no competing interests.

References

Abraham PR, Mulder A, Van 'T Riet J, Raué HA (1994) Characterization of the Saccharomyces cerevisiae nuclear gene CYB3 encoding a cytochrome b polypeptide of respiratory complex II. Molec Gen Genet 242:708–716. https://doi.org/10.1007/BF00283426

Ambati R, Phang S-M, Ravi S, Aswathanarayana R (2014) Astaxanthin: sources, extraction, stability, biological activities and its commercial applications—a review. Mar Drugs 12:128–152. https://doi.org/10.3390/md12010128

An G-H, Cho M-H, Johnson EA (1999) Monocyclic carotenoid biosynthetic pathway in the yeast Phaffia rhodozyma (Xanthophyllomyces dendrorhous). J Biosci Bioeng 88:189–193. https://doi.org/10.1016/S1389-1723(99)80200-X

Bellora N, Moliné M, David-Palma M, Coelho MA, Hittinger CT, Sampaio JP, Gonçalves P, Libkind D (2016) Comparative genomics provides new insights into the diversity, physiology, and sexuality of the only industrially exploited tremellomycete: Phaffia rhodozyma. BMC Genomics 17:901. https://doi.org/10.1186/s12864-016-3244-7

Benesty J, Chen J, Huang Y, Cohen I (2009) Pearson Correlation Coefficient. In: Noise Reduction in Speech Processing. Springer Topics in Signal Processing, vol 2. Springer, Berlin, Heidelberg. https://doi.org/10.1007/978-3-642-00296-0_5

Bereta M, Teplan M, Chafai DE, Radil R, Cifra M (2021) Biological autoluminescence as a noninvasive monitoring tool for chemical and physical modulation of oxidation in yeast cell culture. Sci Rep 11:328. https://doi.org/10.1038/s41598-020-79668-2

Bernard P, Gabarit P, Bahassi EM, Couturier M (1994) Positive-selection vectors using the F plasmid ccdB killer gene. Gene 148:71–74. https://doi.org/10.1016/0378-1119(94)90235-6

Bhatia S, Sharma K, Sharma A, Garg A, Kumar S, Purohit A (2011) Mycosporine and mycosporine-like amino acids: a paramount tool against ultra violet irradiation. Phcog Rev 5:138. https://doi.org/10.4103/0973-7847.91107

Boekhout T, Amend AS, El Baidouri F, Gabaldón T, Geml J, Mittelbach M, Robert V, Tan CS, Turchetti B, Vu D, Wang Q-M, Yurkov A (2022) Trends in yeast diversity discovery. Fungal Divers 114:491–537. https://doi.org/10.1007/s13225-021-00494-6

Bohoyo-Gil D, Dominguez-Valhondo D, García-Parra JJ, González-Gómez D (2012) UHPLC as a suitable methodology for the analysis of carotenoids in food matrix. Eur Food Res Technol 235:1055–1061. https://doi.org/10.1007/s00217-012-1838-0

Breitenbach J, Visser H, Verdoes JC, Van Ooyen AJJ, Sandmann G (2011) Engineering of geranylgeranyl pyrophosphate synthase levels and physiological conditions for enhanced carotenoid and astaxanthin synthesis in Xanthophyllomyces dendrorhous. Biotechnol Lett 33:755–761. https://doi.org/10.1007/s10529-010-0495-2

Brink DP, Mierke F, Norbeck J, Siewers V, Andlid T (2023) Expanding the genetic toolbox of Rhodotorula toruloides by identification and validation of six novel promoters induced or repressed under nitrogen starvation. Microb Cell Fact 22:160. https://doi.org/10.1186/s12934-023-02175-2

Bruchez JJP, Eberle J, Kohler W, Kruft V, Radford A, Russo VEA (1996) bli-4, a gene that is rapidly induced by blue light, encodes a novel mitochondrial, short-chain alcohol dehydrogenase-like protein in Neurospora crassa. Molec Gen Genet 252:223–229. https://doi.org/10.1007/BF02173767

Brych A, Haas FB, Parzefall K, Panzer S, Schermuly J, Altmüller J, Engelsdorf T, Terpitz U, Rensing SA, Kiontke S, Batschauer A (2021) Coregulation of gene expression by White collar 1 and phytochrome in Ustilago maydis. Fungal Genet Biol 152:103570. https://doi.org/10.1016/j.fgb.2021.103570

Cao C, Xue C (2021) More than just cleaning: ubiquitin-mediated proteolysis in fungal pathogenesis. Front Cell Infect Microbiol 11:774613. https://doi.org/10.3389/fcimb.2021.774613

Clum A, Huntemann M, Bushnell B, Foster B, Foster B, Roux S, Hajek PP, Varghese N, Mukherjee S, Reddy TBK, Daum C, Yoshinaga Y, O'Malley R, Seshadri R, Kyrpides NC, Eloe-Fadrosh EA, Chen I-MA, Copeland A, Ivanova NN (2021) DOE JGI metagenome workflow. mSystems 6:e00804-20. https://doi.org/10.1128/mSystems.00804-20

Collins JH, Keating KW, Jones TR, Balaji S, Marsan CB, Çomo M, Newlon ZJ, Mitchell T, Bartley B, Adler A, Roehner N, Young EM (2021) Engineered yeast genomes accurately assembled from pure and mixed samples. Nat Commun 12:1485. https://doi.org/10.1038/s41467-021-21656-9

Da Silva NA, Srikrishnan S (2012) Introduction and expression of genes for metabolic engineering applications in Saccharomyces cerevisiae. FEMS Yeast Res 12:197–214. https://doi.org/10.1111/j.1567-1364.2011.00769.x

Desrivières S, Cooke FT, Parker PJ, Hall MN (1998) MSS4, a phosphatidylinositol-4-phosphate 5-kinase required for organization of the actin cytoskeleton in Saccharomyces cerevisiae. J Biol Chem 273:15787–15793. https://doi.org/10.1074/jbc.273.25.15787

Durmusoglu D, Al'Abri I, Li Z, Islam Williams T, Collins LB, Martínez JL, Crook N (2023) Improving therapeutic protein secretion in the probiotic yeast Saccharomyces boulardii using a multifactorial engineering approach. Microb Cell Fact 22:109. https://doi.org/10.1186/s12934-023-02117-y

England CG, Ehlerding EB, Cai W (2016) NanoLuc: a small luciferase is brightening up the field of bioluminescence. Bioconjugate Chem 27:1175–1187. https://doi.org/10.1021/acs.bioconjchem.6b00112

Galanie S, Thodey K, Trenchard IJ, Filsinger Interrante M, Smolke CD (2015) Complete biosynthesis of opioids in yeast. Science 349:1095–1100. https://doi.org/10.1126/science.aac9373

Gassel S, Schewe H, Schmidt I, Schrader J, Sandmann G (2013) Multiple improvement of astaxanthin biosynthesis in Xanthophyllomyces dendrorhous by a combination of conventional mutagenesis and metabolic pathway engineering. Biotechnol Lett 35:565–569. https://doi.org/10.1007/s10529-012-1103-4

Gasser B, Steiger MG, Mattanovich D (2015) Methanol regulated yeast promoters: production vehicles and toolbox for synthetic biology. Microb Cell Fact 14:196. https://doi.org/10.1186/s12934-015-0387-1

Gerhardt KP, Olson EJ, Castillo-Hair SM, Hartsough LA, Landry BP, Ekness F, Yokoo R, Gomez EJ, Ramakrishnan P, Suh J, Savage DF, Tabor JJ (2016) An open-hardware platform for optogenetics and photobiology. Sci Rep 6:35363. https://doi.org/10.1038/srep35363

Gervasi T, Pellizzeri V, Benameur Q, Gervasi C, Santini A, Cicero N, Dugo G (2018) Valorization of raw materials from agricultural industry for astaxanthin and β-carotene production by Xanthophyllomyces dendrorhous. Nat Prod Res 32:1554–1561. https://doi.org/10.1080/14786419.2017.1385024

Gilchrest BA, Park H, Eller MS, Yaar M (1996) Mechanisms of ultraviolet light-induced pigmentation. Photochem Photobiol 63:1–10. https://doi.org/10.1111/j.1751-1097.1996.tb02988.x

Goldraij A, Curtino JA (1996) M-Glycogenin, the protein moiety of Neurospora crassa proteoglycogen, Is an auto- and transglucosylating enzyme. Biochem Biophys Res Commun 227:909–914. https://doi.org/10.1006/bbrc.1996.1604

Gómez M, Campusano S, Gutiérrez MS, Sepúlveda D, Barahona S, Baeza M, Cifuentes V, Alcaíno J (2020) Sterol regulatory element-binding protein Sre1 regulates carotenogenesis in the red yeast Xanthophyllomyces dendrorhous. J Lipid Res 61:1658–1674. https://doi.org/10.1194/jlr.RA120000975

Hahn S, Guarente L (1988) Yeast HAP2 and HAP3: Transcriptional activators in a heteromeric complex. Science 240:317–321. https://doi.org/10.1126/science.2832951

Hara KY, Morita T, Endo Y, Mochizuki M, Araki M, Kondo A (2014) Evaluation and screening of efficient promoters to improve

astaxanthin production in Xanthophyllomyces dendrorhous. Appl Microbiol Biotechnol 98:6787–6793. https://doi.org/10.1007/s00253-014-5727-2

Hong K-K, Nielsen J (2012) Metabolic engineering of Saccharomyces cerevisiae: a key cell factory platform for future biorefineries. Cell Mol Life Sci 69:2671–2690. https://doi.org/10.1007/s00018-012-0945-1

Huang R, Ding R, Liu Y, Li F, Zhang Z, Wang S (2022) GATA transcription factor WC2 regulates the biosynthesis of astaxanthin in yeast Xanthophyllomyces dendrorhous. Microb Biotechnol 15:2578–2593. https://doi.org/10.1111/1751-7915.14115

Iverson SV, Haddock TL, Beal J, Densmore DM (2016) CIDAR MoClo: improved MoClo assembly standard and new E. coli part library enable rapid combinatorial design for synthetic and traditional biology. ACS Synth Biol 5:99–103. https://doi.org/10.1021/acssynbio.5b00124

Karim AS, Curran KA, Alper HS (2013) Characterization of plasmid burden and copy number in Saccharomyces cerevisiae for optimization of metabolic engineering applications. FEMS Yeast Res 13:107–116. https://doi.org/10.1111/1567-1364.12016

Kim D, Langmead B, Salzberg SL (2015) HISAT: a fast spliced aligner with low memory requirements. Nat Methods 12:357–360. https://doi.org/10.1038/nmeth.3317

Lai J, Liu W, Bu J, Chen X, Hu B, Zhu M (2023) Enhancement of astaxanthin production from food waste by Phaffia rhodozyma screened by flow cytometry and feed application potential. Biotechol Appl Biochem 70:1817–1829. https://doi.org/10.1002/bab.2484

Ledetzky N, Osawa A, Iki K, Pollmann H, Gassel S, Breitenbach J, Shindo K, Sandmann G (2014) Multiple transformation with the crtYB gene of the limiting enzyme increased carotenoid synthesis and generated novel derivatives in Xanthophyllomyces dendrorhous. Arch Biochem Biophys 545:141–147. https://doi.org/10.1016/j.abb.2014.01.014

Li W, Cui L, Mai J, Shi T-Q, Lin L, Zhang Z-G, Ledesma-Amaro R, Dong W, Ji X-J (2022) Advances in metabolic engineering paving the way for the efficient biosynthesis of terpenes in yeasts. J Agric Food Chem 70:9246–9261. https://doi.org/10.1021/acs.jafc.2c03917

Li W, Luna-Flores CH, Anangi R, Zhou R, Tan X, Jessen M, Liu L, Zhou R, Zhang T, Gissibl A, Cullen PJ, Ostrikov KK, Speight RE (2023) Oxidative stress induced by plasma-activated water stimulates astaxanthin production in *Phaffia* rhodozyma. Bioresour Technol 369:128370. https://doi.org/10.1016/j.biortech.2022.128370

Liao Y, Smyth GK, Shi W (2014) featureCounts: an efficient general purpose program for assigning sequence reads to genomic features. Bioinform 30:923–930. https://doi.org/10.1093/bioinformatics/btt656

Libkind D, Ruffini A, Van Broock M, Alves L, Sampaio JP (2007) Biogeography, host specificity, and molecular phylogeny of the basidiomycetous yeast Phaffia rhodozyma and its sexual form, Xanthophyllomyces dendrorhous. Appl Environ Microbiol 73:1120–1125. https://doi.org/10.1128/AEM.01432-06

Libkind D, Peris D, Cubillos FA, Steenwyk JL, Opulente DA, Langdon QK, Rokas A, Hittinger CT (2020) Into the wild: new yeast genomes from natural environments and new tools for their analysis. FEMS Yeast Res 20:foaa008. https://doi.org/10.1093/femsyr/foaa008

Llewellyn CA, Greig C, Silkina A, Kultschar B, Hitchings MD, Farnham G (2020) Mycosporine-like amino acid and aromatic amino acid transcriptome response to UV and far-red light in the cyanobacterium Chlorogloeopsis fritschii PCC 6912. Sci Rep 10:20638. https://doi.org/10.1038/s41598-020-77402-6

Löbs A-K, Schwartz C, Wheeldon I (2017) Genome and metabolic engineering in non-conventional yeasts: current advances and applications. Synth Syst Biotechnol 2:198–207. https://doi.org/10.1016/j.synbio.2017.08.002

Loto I, Gutiérrez MS, Barahona S, Sepúlveda D, Martínez-Moya P, Baeza M, Cifuentes V, Alcaíno J (2012) Enhancement of carotenoid production by disrupting the C22-sterol desaturase gene (CYP61) in Xanthophyllomyces dendrorhous. BMC Microbiol 12:235. https://doi.org/10.1186/1471-2180-12-235

Love MI, Huber W, Anders S (2014) Moderated estimation of fold change and dispersion for RNA-seq data with DESeq2. Genome Biol 15:550. https://doi.org/10.1186/s13059-014-0550-8

Luna-Flores CH, Wang A, Cui Z, von Hellens J, Speight RE (2022) Towards commercial levels of astaxanthin production in Phaffia rhodozyma. J Biotechnol 350:42–54. https://doi.org/10.1016/j.jbiotec.2022.04.001

Luo W, Friedman MS, Shedden K, Hankenson KD, Woolf PJ (2009) GAGE: generally applicable gene set enrichment for pathway analysis. BMC Bioinformatics 10:161. https://doi.org/10.1186/1471-2105-10-161

Manni M, Berkeley MR, Seppey M, Zdobnov EM (2021a) BUSCO: assessing genomic data quality and beyond. Protoc 1:1–41. https://doi.org/10.1002/cpz1.323

Manni M, Berkeley MR, Seppey M, Simão FA, Zdobnov EM (2021b) BUSCO update: novel and streamlined workflows along with broader and deeper phylogenetic coverage for scoring of eukaryotic, prokaryotic, and viral genomes. Mol Biol Evol 38:4647–4654. https://doi.org/10.1093/molbev/msab199

Merényi Z, Krizsán K, Sahu N, Liu X-B, Bálint B, Stajich JE, Spatafora JW, Nagy LG (2023) Genomes of fungi and relatives reveal delayed loss of ancestral gene families and evolution of key fungal traits. Nat Ecol Evol 7:1221–1231. https://doi.org/10.1038/s41559-023-02095-9

Mülleder M, Capuano F, Pir P, Christen S, Sauer U, Oliver SG, Ralser M (2012) A prototrophic deletion mutant collection for yeast metabolomics and systems biology. Nat Biotechnol 30:1176–1178. https://doi.org/10.1038/nbt.2442

Mussagy CU, Santos-Ebinuma VC, Herculano RD, Coutinho JAP, Pereira JFB, Pessoa A (2022) Ionic liquids or eutectic solvents? Identifying the best solvents for the extraction of astaxanthin and β-carotene from Phaffia rhodozyma yeast and preparation of biodegradable films. Green Chem 24:118–123. https://doi.org/10.1039/D1GC03521E

Naguib YMA (2000) Antioxidant activities of astaxanthin and related carotenoids. J Agric Food Chem 48:1150–1154. https://doi.org/10.1021/jf991106k

Nagy LG, Ohm RA, Kovács GM, Floudas D, Riley R, Gácser A, Sipiczki M, Davis JM, Doty SL, De Hoog GS, Lang BF, Spatafora JW, Martin FM, Grigoriev IV, Hibbett DS (2014) Latent homology and convergent regulatory evolution underlies the repeated emergence of yeasts. Nat Commun 5:4471. https://doi.org/10.1038/ncomms5471

Olmedo M, Ruger-Herreros C, Luque EM, Corrochano LM (2010) A complex photoreceptor system mediates the regulation by light of the conidiation genes Con-10 and Con-6 in Neurospora crassa. Fungal Genet Biol 47:352–363. https://doi.org/10.1016/j.fgb.2009.11.004

Otoupal PB, Ito M, Arkin AP, Magnuson JK, Gladden JM, Skerker JM (2019) Multiplexed CRISPR-Cas9-based genome editing of Rhodosporidium toruloides. mSphere 4:e00099-19. https://doi.org/10.1128/mSphere.00099-19

Overbeek R (2003) The ERGOTM genome analysis and discovery system. Nucleic Acids Res 31:164–171. https://doi.org/10.1093/nar/gkg148

Pelletier H, Kraut J (1992) Crystal structure of a complex between electron transfer partners, cytochrome c peroxidase and cytochrome c. Science 258:1748–1755. https://doi.org/10.1126/science.1334573

Peris D, Ubbelohde EJ, Kuang MC, Kominek J, Langdon QK, Adams M, Koshalek JA, Hulfachor AB, Opulente DA, Hall DJ, Hyma

K, Fay JC, Leducq J-B, Charron G, Landry CR, Libkind D, Gonçalves C, Gonçalves P, Sampaio JP, Wang Q-M, Bai F-Y, Wrobel RL, Hittinger CT (2023) Macroevolutionary diversity of traits and genomes in the model yeast genus Saccharomyces. Nat Commun 14:690. https://doi.org/10.1038/s41467-023-36139-2

Rahman F, Hassan M, Hanano A, Fitzpatrick DA, McCarthy CGP, Murphy DJ (2018) Evolutionary, structural and functional analysis of the caleosin/peroxygenase gene family in the fungi. BMC Genomics 19:976. https://doi.org/10.1186/s12864-018-5334-1

Rakhmanova TI, Sekova VYu, Gessler NN, Isakova EP, Deryabina YI, Popova TN, Shurubor YI, Krasnikov BF (2023) Kinetic and regulatory properties of Yarrowia lipolytica aconitate hydratase as a model-indicator of cell redox state under pH stress. IJMS 24:7670. https://doi.org/10.3390/ijms24087670

Rodríguez-Sáiz M, Godio RP, Álvarez V, De La Fuente JL, Martín JF, Barredo JL (2009) The NADP-dependent glutamate dehydrogenase gene from the astaxanthin producer Xanthophyllomyces dendrorhous: use of its promoter for controlled gene expression. Mol Biotechnol 41:165–172. https://doi.org/10.1007/s12033-008-9123-y

Santopietro LMD, Spencer JFT, Spencer DM, Siñeriz F (1998) Effects of oxidative stress on the production of carotenoid pigments by Phaffia rhodozyma (Xanthophyllomyces dendrorhous). Folia Microbiol 43:173–176. https://doi.org/10.1007/BF02816505

Schwartz C, Shabbir-Hussain M, Frogue K, Blenner M, Wheeldon I (2017) Standardized markerless gene integration for pathway engineering in Yarrowia lipolytica. ACS Synth Biol 6:402–409. https://doi.org/10.1021/acssynbio.6b00285

Schwarzhans J-P, Wibberg D, Winkler A, Luttermann T, Kalinowski J, Friehs K (2016) Non-canonical integration events in Pichia pastoris encountered during standard transformation analysed with genome sequencing. Sci Rep 6:38952. https://doi.org/10.1038/srep38952

Serafini DM, Schellhorn HE (1999) Endonuclease III and endonuclease IV protect Escherichia coli from the lethal and mutagenic effects of near-UV irradiation. Can J Microbiol 45:632–637. https://doi.org/10.1139/w99-039

Sharma R, Gassel S, Steiger S, Xia X, Bauer R, Sandmann G, Thines M (2015) The genome of the basal agaricomycete Xanthophyllomyces dendrorhous provides insights into the organization of its acetyl-CoA derived pathways and the evolution of Agaricomycotina. BMC Genomics 16:233. https://doi.org/10.1186/s12864-015-1380-0

Shin J, South EJ, Dunlop MJ (2022) Transcriptional tuning of mevalonate pathway enzymes to identify the impact on limonene production in Escherichia coli. ACS Omega 7:18331–18338. https://doi.org/10.1021/acsomega.2c00483

Sinha RP, Häder D-P (2002) UV-induced DNA damage and repair: a review. Photochem Photobiol Sci 1:225–236. https://doi.org/10.1039/b201230h

Smythe C, Cohen P (1991) The discovery of glycogenin and the priming mechanism for glycogen biogenesis. Eur J Biochem 200:625–631. https://doi.org/10.1111/j.1432-1033.1991.tb16225.x

Stachowiak B (2013) Effect of illumination intensities on astaxanthin synthesis by Xanthophyllomyces dendrorhous and its mutants. Food Sci Biotechnol 22:1033–1038. https://doi.org/10.1007/s10068-013-0180-z

Stanke M, Keller O, Gunduz I, Hayes A, Waack S, Morgenstern B (2006) AUGUSTUS: ab initio prediction of alternative transcripts. Nucleic Acids Res 34:W435–W430. https://doi.org/10.1093/nar/gkl200

Steensels J, Verstrepen KJ (2014) Taming wild yeast: potential of conventional and nonconventional yeasts in industrial fermentations. Annu Rev Microbiol 68:61–80. https://doi.org/10.1146/annurev-micro-091213-113025

Storebakken T, Sørensen M, Bjerkeng B, Hiu S (2004) Utilization of astaxanthin from red yeast, Xanthophyllomyces dendrorhous, in rainbow trout, Oncorhynchus mykiss: effects of enzymatic cell wall disruption and feed extrusion temperature. Aquaculture 236:391–403. https://doi.org/10.1016/j.aquaculture.2003.10.035

Toplak M, Brunner J, Tabib CR, Macheroux P (2019) Closing the gap: yeast electron-transferring flavoprotein links the oxidation of D-lactate and D-α-hydroxyglutarate to energy production via the respiratory chain. FEBS J 286:3611–3628. https://doi.org/10.1111/febs.14924

Tropea A, Gervasi T, Melito MR, Curto AL, Curto RL (2013) Does the light influence astaxanthin production in Xanthophyllomyces dendrorhous ? Nat Prod Res 27:648–654. https://doi.org/10.1080/14786419.2012.688045

Vázquez M (2001) Effect of the light on carotenoid profiles of Xanthophyllomyces dendrorhous strains (formerly Phaffia rhodozyma). Food Technol Biotechnol 39:123–128

Visser H, Sandmann G, Verdoes JC (2005) Xanthophylls in fungi. In: Barredo JL (ed) Microbial processes and products. Methods in biotechnology, 18. Humana Press, Totowa, NJ, pp 257–272. https://doi.org/10.1385/1-59259-847-1:257

Wagner JM, Alper HS (2016) Synthetic biology and molecular genetics in non-conventional yeasts: current tools and future advances. Fungal Genet Biol 89:126–136. https://doi.org/10.1016/j.fgb.2015.12.001

Wery J, Gutker D, Renniers ACHM, Verdoes JC, Van Ooyen AJJ (1997) High copy number integration into the ribosomal DNA of the yeast Phaffia rhodozyma. Gene 184:89–97. https://doi.org/10.1016/S0378-1119(96)00579-3

Yaguchi A, Rives D, Blenner M, Department of Chemical and Biomolecular Engineering, Clemson University, Clemson SC 29634, USA (2017) New kids on the block: emerging oleaginous yeast of biotechnological importance. AIMS Microbiol 3:227–247. https://doi.org/10.3934/microbiol.2017.2.227

Yamamoto K, Hara KY, Morita T, Nishimura A, Sasaki D, Ishii J, Ogino C, Kizaki N, Kondo A (2016) Enhancement of astaxanthin production in Xanthophyllomyces dendrorhous by efficient method for the complete deletion of genes. Microb Cell Fact 15:155. https://doi.org/10.1186/s12934-016-0556-x

Young EM, Zhao Z, Gielesen BEM, Wu L, Benjamin Gordon D, Roubos JA, Voigt CA (2018) Iterative algorithm-guided design of massive strain libraries, applied to itaconic acid production in yeast. Metab Eng 48:33–43. https://doi.org/10.1016/j.ymben.2018.05.002

Yu Z, Fischer R (2019) Light sensing and responses in fungi. Nat Rev Microbiol 17:25–36. https://doi.org/10.1038/s41579-018-0109-x

Zahrl RJ, Peña DA, Mattanovich D, Gasser B (2017) Systems biotechnology for protein production in Pichia pastoris. FEMS Yeast Res 17:7. https://doi.org/10.1093/femsyr/fox068

Zeevi D, Lubliner S, Lotan-Pompan M, Hodis E, Vesterman R, Weinberger A, Segal E (2014) Molecular dissection of the genetic mechanisms that underlie expression conservation in orthologous yeast ribosomal promoters. Genome Res 24:1991–1999. https://doi.org/10.1101/gr.179259.114

Authors and Affiliations

Emma E. Tobin[1] · Joseph H. Collins[1] · Celeste B. Marsan[1] · Gillian T. Nadeau[1] · Kim Mori[1] · Anna Lipzen[2] · Stephen Mondo[2] · Igor V. Grigoriev[2,3] · Eric M. Young[1]

✉ Eric M. Young
ericyoung7@gmail.com

[1] Life Sciences and Bioengineering Center, Department of Chemical Engineering, Worcester Polytechnic Institute, Worcester, MA, USA

[2] U.S. Department of Energy Joint Genome Institute, Lawrence Berkeley National Laboratory, Berkeley, CA 94720, USA

[3] Plant and Microbial Biology, University of California Berkeley, Berkeley, CA 94720, USA